Photoacoustic spectroscopy of magnetic fluids

A.C. Oliveira[a,*], A.L. Tronconi[a], N. Buske[b], P.C. Morais[a]

[a] *Instituto de Física, Universidade de Brasília, DF 70919-970 Brasília, Brazil*
[b] *Berlin Heart AG, Wiesenweg 10, D-12247 Berlin, Germany*

Abstract

In this study photoacoustic spectroscopy is introduced as a promising experimental technique to investigate magnetic fluids (MFs). The spectral features of representative uncoated- and coated MFs in the 0.3–1.0 μm wavelength region have been discussed and identified in terms of three distinct bands (L, S, and C). Band-L in the spectral range 0.65–0.90 μm was ascribed to the characteristic coating layer of the magnetic nanoparticle. Band-S occurring around 0.47 μm was ascribed to the metal-poly oxy-hydroxy surface layer built up at the nanoparticle surface. Finally, band-C has been associated to the optical band edge absorption of the semiconductor magnetic nanoparticle. Fe_3O_4 nanoparticles (9.4 nm diameter) and $CoFe_2O_4$ nanoparticles (4.3 and 11.4 nm diameter) were used as core materials in the coated- and uncoated-MF samples, respectively.
© 2002 Elsevier Science B.V. All rights reserved.

Keywords: Magnetic fluids; Photoacoustic spectroscopy

High-resolution microscopy [1], magnetization measurements [2], and static magnetic birefringence [3] are traditional magnetic fluid (MF) characterization techniques. Magnetic resonance [4] and Raman spectroscopy [5] were introduced more recently as valuable tools in the investigation of MFs. However, the wide range of applications of such material system, as for instance in the biomedical field, requires a more detailed investigation of the MF properties; in particular, the nature and interaction of the nanoparticle surface coating layer with the surrounding medium. Photoacoustic (PA) spectroscopy is a surface-based, well-established experimental technique [6], though it has never been used to investigate MF samples. Briefly, the PA effect measures the nonradiative deexcitation processes that occur in a system after it has been optically excited. In this study we are proposing the use of the PA signal obtained from thin liquid films of MFs deposited on top of inert substrates to draw conclusion about the properties of the magnetic nanoparticles and the surface-coating layer.

Ferrite-based MF samples used in this study were obtained by co-precipitating bivalent (Fe^{2+} and Co^{2+}) and the trivalent (Fe^{3+}) transition metal-ions in alkaline medium in order to produce magnetic nanoparticles, following two distinct surface treatments. Two different coating agents were used to produce coated-MF (CMF) samples based on Fe_3O_4 nanoparticles with mean diameter value of 9.4 nm [7]. The coating agents were oleoylsarcosine (CMF1 sample) and lauric acid (CMF2 sample). Coating with oleoylsarcosine was used to produce the water-based CMF1 sample, while double coating with lauric acid was used to produce the water-based CMF2 sample. Two preparations containing $CoFe_2O_4$ nanoparticles with different mean diameter values (4.3 and 11.4 nm) were used to produce water-based uncoated-MF (UMF) samples [8]. The $CoFe_2O_4$-UMF samples were stabilized around pH 3 and labeled UMF1 and UMF2 corresponding to mean diameter values of 4.3 and 11.4 nm, respectively. PA spectra were taken from the four MF samples prepared as a thin liquid film on top of a polished quartz substrate. The MF samples were enclosed in a sealed, high-performance, PA cell at atmospheric pressure, coupled to a sensitive microphone. Details of the homemade PA cell will be published elsewhere. The light from a 150 W Xe

---

lamp was dispersed by a 0.22 m double monochromator (Spex model 1680) and used as the variable wavelength light source. The light was chopped at a frequency of a few hertz, to improve the signal/noise ratio. Several PA features were observed in the wavelength range of our investigation (0.3–1 μm). An intense band (band-C) was observed in the range 0.35–0.45 μm in all MF samples. A less intense structure (band-S) was observed around 0.47 μm, which is stronger in UMF samples in comparison to the CMF samples. Finally, in the 0.65–0.90 μm region a complex structure (band-L), different in the two groups of samples investigated (CMFs and UMFs), was observed. The PA spectra of each MF sample were investigated as a function of time, up to about 200 h after sample preparation for PA measurements.

Fig. 1 shows the PA spectra of the CMF and UMF samples in the range 0.3–1 μm. The features occurring in bands L, S, and C will be discussed as follows. Band-L shows similar features in all ferrite-based UMF samples we have investigated so far, including samples with divalent metal-ions as different as Fe^{2+}, Mn^{2+}, Co^{2+}, Ni^{2+}, Zn^{2+}, and Cu^{2+} (data not shown). Different from the UMF samples, band-L in CMF samples shows similar features in all magnetite-based CMF samples we have investigated so far, including water- and hydrocarbon-based MF samples (data not shown). We claim that band-L is related to the characteristics of the MF

stabilizing coating layer, thus explaining the differences observed in the PA spectra of UMF and CMF samples shown in Fig. 1. While the main peak (around 0.47 μm) of band-S is quite intense in cobalt ferrite-based UMF samples it is observed as a tiny shoulder in the CMF2 sample and it is almost absent in the sample CMF1. We claim that band-S is related to the metal-poly oxyhydroxy surface layer built up at the ferrite-based nanoparticle surface, which is particularly enriched by hydroxyl groups [9]. The strong peak around 0.47 μm, observed in the UMF samples investigated, indicates the expected high-surface hydroxyl-grafting coefficient. Note that the PA peak around 0.47 μm is typical of the crystal field band of Co^{2+} ions in a distorted octahedral environment [10]. In contrast, the lower surface-grafting coefficient associated to hydroxyl groups in CMF samples are in very good agreement with the weak PA signal intensity of the main feature in band-S. The absence of the main PA peak around 0.47 μm in sample CMF1 indicates the relative highest grafting coefficient of oleoylsarcosine in comparison to the double dodecanoic acid. Indeed, the spectral features observed in band-L and -S could be associated to higher-order Raman overtones due to molecular species in the coating layer and in the nanoparticle surface, respectively.

While band-L and -S have been, respectively, ascribed to the stabilizing coating layer and the nanoparticle surface layer, band-C is more likely to be related to the absorption of the incident light by the core nanoparticle. At this point we should mention that the PA signal scales with the optical absorption coefficient and, under low optical excitation intensities, the PA signal scales linearly with the optical absorption coefficient. Further, the optical absorption edge of most bulk ferrite-based crystals is in the range 0.3–0.4 μm [10]. It is important to mention that a semiconductor quantum dot model has been successfully used to explain the charge–discharge mechanism as well as the stability of aqueous colloids based on ferrite nanoparticles [11]. Therefore, the main feature of band-C in the PA spectra shown in Fig. 1, particularly the rapid raise of the PA signal at decreasing wavelength, may be the signature of optical processes near the semiconductor absorption edge. Indeed, the PA feature of band-C has been previously refereed to a charge-transfer band [12]. It should be observed from Fig. 1 that band-C peaks at lower wavelength for CMF samples than for UMF samples. Such result reflects the higher-energy absorption edge for Fe_3O_4-based nanoparticles than for $CoFe_2O_4$-based nanoparticles. Even more significant is the energy shift observed in the main peak of band-C when comparing sample UMF1 with sample UMF2 (see Fig. 1). While the main peak in band-C peaks around 0.378 μm for sample UMF1, it occurs around 0.388 μm in sample UMF2. Such energy up-shift of band-C in sample UMF1 in comparison with
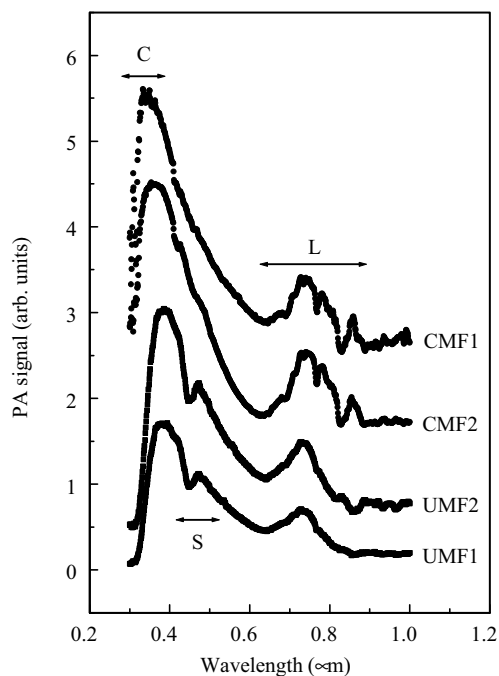

Fig. 1. PA spectra of the two $CoFe_2O_4$-UMF samples (UMF1 and UMF2) and the two Fe_3O_4-CMF samples (CMF1 and CMF2).

sample UMF2 could be explained by the increase of the effective band-gap due to the stronger quantum confinement in sample UMF1, as a result of the smaller particle size (4.3 nm diameter). From the point of view of PA spectroscopy, including here aspects related to sample preparation for PA measurements, we found relevant the investigation of the PA spectrum as a function of time. The PA spectra (not shown) of sample CMF2 right after sample preparation (0 h) as well as at five distinct times (27, 68, 148, 166, and 195 h) reveal that all the main spectral features ascribed to L, S, and C bands are fully preserved.

In summary, PA spectroscopy is for the first time used in the investigation of thin films of MFs. Several features were identified in the 0.3–1 μm spectral range. In particular, in the coated- and uncoated MFs three distinct bands (L, S, and C) investigated were identified in the range of our investigation. Bands L, S, and C were ascribed to the coating layer, the metal-poly oxy-hydroxy thin layer at the nanoparticle surface, and the core nanoparticle itself, respectively.

References

[1] B.M. Lacava, R.B. Azevedo, L.P. Silva, Z.G.M. Lacava, K. Skeff Neto, N. Buske, A.F. Bakuzis, P.C. Morais, Appl. Phys. Lett. 77 (2000) 1876.

[2] P.C. Morais, C.B. Teixeira, K. Skeff Neto, R.B. Azevedo, Z.G.M. Lacava, L.M. Lacava, Solid State Commun. 114 (2000) 59.

[3] K. Skeff Neto, A.F. Bakuzis, P.C. Morais, A.R. Pereira, R.B. Azevedo, L.M. Lacava, Z.G.M. Lacava, J. Appl. Phys. 89 (2001) 3362.

[4] G.R.R. Gonçalves, A.R. Pereira, A.F. Bakuzis, P.C. Morais, F. Pelegrini, K. Skeff Neto, J. Magn. Magn. Mater. 226–230 (2001) 1896.

[5] P.C. Morais, S.W. da Silva, M.A.G. Soler, N. Buske, J. Phys. Chem. A 104 (2000) 2894.

[6] A. Rosencwaig, A. Gersho, Science 190 (1975) 556.

[7] D. Gunther, N. Buske, DE Patent 4325386, 1993.

[8] P.C. Morais, V.K. Garg, A.C. Oliveira, L.P. Silva, R.B. Azevedo, A.M.L. Silva, E.C.D. Lima, J. Magn. Magn. Mater. 225 (2001) 37.

[9] P.C. Morais, S.W. da Silva, M.A.G. Soler, N. Buske, Biomol. Eng. 17 (2001) 41.

[10] Y.-M. Chiang, D. Birnie III, W.D. Kingery, Physical Ceramics: Principles for Ceramic Science and Engineering, Wiley, New York, 1997.

[11] Fanyao Qu, P.C. Morais, J. Phys. Chem. B 104 (2000) 5232.

[12] A. Rosencwaig, Solid state photoacoustic spectroscopy, in: Y.-H. Pao (Ed.), Optoacoustic Spectroscopy and Detection, Academic Press, New York, 1977, p. 193.